

Analytical Investigation on Seismic Behavior of Inverted V-braced Frames

Hee-Jin Yeom¹ and Jung-Han Yoo^{2,*}

¹Master of Science, School of Architecture, Seoul National University of Science & Technology, 01811, Seoul, Korea

²Associate Professor, School of Architecture, Seoul National University of Science & Technology, 01811, Seoul, Korea

Abstract

An inverted V-braced frame is one of the most widely used CBFs (Concentrically Braced Frames) owing to many advantages in constructional design. The seismic behaviors of inverted V-braced frames is that brace buckling occurs due to strong motion generation, and that in turn vertical unbalanced force is created between tension brace and compression brace, resulting in an additional load onto beams. Thus, members of beams should be designed to have enough strength to ensure plastic hinge is not created. In this study, a series of finite element analysis was conducted to evaluate the earthquake-resistant performances of the methods to design the clearance distance of gusset plates in inverted V-braced frames, and to evaluate vertical unbalanced force depending on the cross-section size of beams. It was found that the results of the equation of vertical unbalanced force in the current standards were more conservative than the load generated through the real analysis model. In addition, the model of designing elliptical clearance distance showed higher earthquake-resistant performances than that of designing linear clearance distance, which requires the reconsideration and improvement of the current practices of calculating vertical unbalanced force and setting clearance distance.

Keywords: inverted V-braced frames, gusset plate connections, inelastic behavior, finite element model, cyclic loading, vertical unbalanced force

1. Introduction

Until the Northridge earthquake in 1994 and the Kobe earthquake in 1995, building construction experts used to think that “steel structures are safe from earthquake because of the ductility capacity of steel materials themselves.” However, the two earthquakes caused huge damage to buildings with steel structures, and it was found to be mostly attributable to connection failure caused by brittle fracture of welded structures. That is, unless a balance between connection designs and the strength of frame members is secured to ensure the inherent ductility capacity of structural materials is well exhibited, structures can never be safe.

A braced frame is an earthquake-resistant design system of steel-frame structures, and thanks to its high rigidity and strength, as well as economic feasibility, it is widely used in strong motion generation areas and frequent earthquake areas. Braces of concentrically braced frames

(CBFs) that are used in capacity design methods are subject to deformations caused by repeated tension and compression after buckling, and through this behavior, seismic energy is dissipated. To achieve this behavior, restraint-free plastic rotations should be allowed for a gusset plate to have flexible brace end conditions, which requires sufficient free length (clearance distance) between the end of the brace member and the restrained line of the gusset plate, but short enough to preclude the occurrence of buckling in the gusset plate before brace buckling.

CBFs are divided, depending on the shapes of braces, into brace frame, X-braced frame, and V-braced and inverted V-braced frames. Inverted V-braced frames are widely used owing to many advantages in constructional design. In addition to the beam-column connection, another gusset plate should be placed at the middle of a beam due to its geometric characteristics. Under earthquake, compression and tension brace forces coexist in inverted V-braced frames. Compression brace force starts to decrease after buckling, while tension brace force continues to increase until it reaches full tension yield, which results in unbalanced forces between the two braces. Since this creates the vertical unbalanced force in the beam, and in turn imposes additional loads, this should be considered in designing members.

Received February 17, 2017; accepted July 13, 2017;
published online March 31, 2018
© KSSC and Springer 2018

*Corresponding author
E-mail: happyjh@seoultech.ac.kr

Thus, in this study, the failure mode, yield mechanism and overall behavior of inverted V-braced frames were evaluated using finite element analysis methods. As mentioned above, axial force and post-buckling strength imposed on each of tension and compression braces were analyzed, and the vertical unbalanced force acquired from the equation of the current standard (AISC, 2010a) was compared with the vertical unbalanced force that is actually created in the analysis model. It was analyzed how the size of cross sections affects earthquake-resistant performances of the frame by varying the cross section of beams to which additional bending and shear force are applied by vertical unbalanced force. Earthquake-resistant performances were also evaluated by comparing the difference of earthquake-resistant behaviors of inverted V-braced frames depending on the methods of calculating the clearance distance of gusset plate connections.

2. Current AISC Design Provisions for V-braced Frames

2.1. Vertical unbalanced force

The influence of unequal compression and tension brace forces on the behavior of V- and inverted V-braced frames has long been recognized (Khatib *et al.*, 1988). If improperly accounted for, the resulting unbalanced force can negatively influence behavior of the beams, and in-turn lead to undesirable plastic collapse mechanisms. Figure 1 illustrated this concept for a simple frame (Bruneau *et al.*, 2011). Once the buckling strength of the compression brace is reached, any additional increase in the lateral load, V , is entirely resisted by the brace in tension. The difference in the vertical and horizontal component of the forces results in vertical unbalanced load, P_{un-u} and unbalanced horizontal load, P_{un-h} , applied to the beam at the beam-to-brace intersection point:

$$P_{un-u} = (T - C)\sin\theta \tag{1}$$

$$P_{un-h} = (T + C)\cos\theta \tag{2}$$

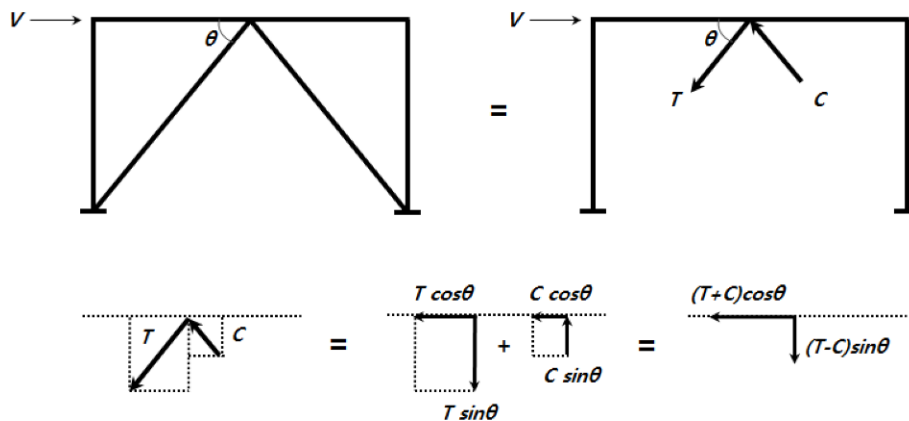


Figure 1. Forces acting on beam of inverted V-braced frame due to unbalanced resistance (Bruneau *et al.*, 2011).

Based on this theory, the current AISC Seismic Provisions (2010b) requires that vertical unbalanced force shall be calculated as follows:

The required strength shall be determined based on the load combinations of the applicable building code assuming that the braces provide no support of dead and live loads. For load combinations that include earthquake effects, the seismic load effect on the member shall be determined as follows:

(i) The forces in braces in tension shall be assumed to be the least of the following:

(a) The expected yield strength of the brace in tension, $R_u F_y A_o$

(b) The load effect based upon the amplified seismic load

(c) The maximum force that can be developed by the system

(ii) The forces in braces in compression shall be assumed to be equal to $0.3P_n$.

The vertical unbalanced force for design (V_u) is then computed by using Eq. (3) as follows:

$$V_u = (R_u F_y A_o - 0.3P_n)\sin\theta \tag{3}$$

2.2. Connection design

For brace buckling out of plane of single plate gussets, weak-axis bending in the gusset is induced by member end rotations. This results in flexible end conditions with plastic hinges at mid-span in addition to the hinges that form in the gusset plate. This requires that the free length between the end of the brace and the assumed line of restraints for the gusset be sufficiently long to permit plastic rotations, yet short enough to preclude the occurrence of plate buckling prior to member buckling. A length of two times the plate thickness, $2t_n$ linear clearance, is recommended, as illustrated in Fig. 2(a) (AISC, 2010a; Astaneh-asl *et al.*, 1986).

Recent studies have shown that the $2t_n$ linear clearance often results in relatively large, thick gusset plates.

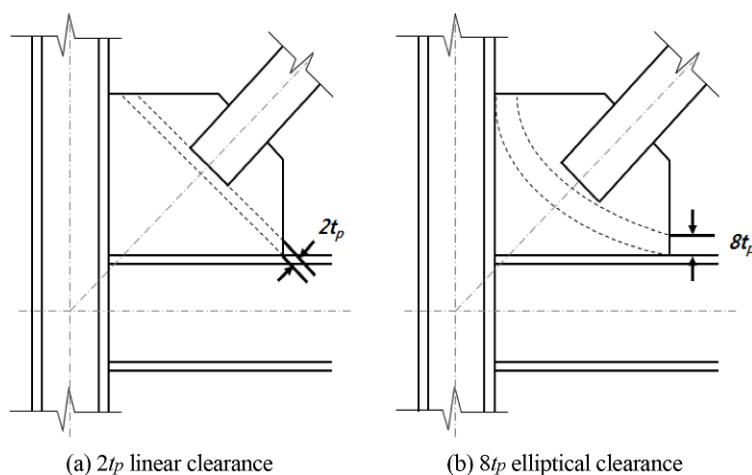


Figure 2. Schematic of concentrically braced frame gusset plate connections.

Observations from nonlinear analyses and experiments showed that a more compact gusset plate can achieve the brace end rotation demands and reduce construction challenges. Using those results as a basis, an alternative elliptical clearance method was developed for corner gusset plates, as indicated in Fig. 2(b) (Lehman *et al.*, 2008; Roeder *et al.*, 2011).

3. Descriptions of Experimental and Analytical Models

3.1. Test frame

To verify the finite element analysis model that would be used in this study, the results of the inverted V-braced frame test that was conducted in Japan was used (Okazaki *et al.*, 2013). Figure 3(a) shows an elevation of the CBF (Concentrically Braced Frame) specimen. The centerline measurements of the specimen were 4.15-m span by 2.25-m height which corresponds to 70% scale of typical building structures. The test specimen consisted of a beam, two columns, two braces and three gusset plate connections, as illustrated in Fig. 3(a). Table 1 indicates the dimensions and the measured material properties of the specimen. The gusset plates did not represent current design provisions. The three gusset plates were designed according to the balanced design proposed by Lehman *et al.* (2008) and Roeder *et al.* (2011); by adopting an elliptical clearance distance of eight times the thickness of the gusset plate, as referred to earlier.

The columns were rigidly connected to heavy base beams, which in turn were rigidly connected to the test-bed system. The test beds are multipurpose devices that supply horizontal mass to the each side of the beam. The specimen was laterally restrained along the columns and beam at discrete locations indicated in Fig. 3(a) by \times marks (Okazaki *et al.*, 2013). At the bottom of the specimen, the east-west component of the JR Takatori motion (Nakamura *et al.*, 1996) was introduced in the

direction parallel to the shaking table. The JR Takatori motion is a strong motion record from the 1995 Kobe earthquake, measured immediately adjacent to the fault. Figure 4 shows the acceleration history of the motion. The shaking table tests were conducted by introducing the Takatori EW motion seven times, with the target amplification level increasing from 10, 12, 14, 28, 28, 42, and finally, to 70% (Okazaki *et al.*, 2013).

3.2. Analytical model

A comprehensive series of nonlinear, inelastic finite-element (FE) analyses were performed to simulate the response of the test specimen using ANSYS (2012). The FE model was constructed using four-node quadrilateral shell elements for all of the members (SHELL181). The four-node element has 6 degrees of freedom at each node, specifically translations and rotations in the x , y , and z directions. A large-displacement formulation was used to simulate buckling and a bilinear kinematic hardening plastic material model was adopted to simulate the inelastic behavior of steel under cyclic loading. The measured material properties were used in the analyses (Table 1).

Figure 3(b) shows the FE model configuration and boundary conditions. All restraints indicated in Fig. 3(b) were applied to simulate the experimental boundary conditions. Load history was applied to the loading plane of the analysis model by dividing the maximum displacement by a certain increment based on 70% of the JR Takatori ground motion. For the initial imperfection length of the middle of the brace, a residual out-of-plane displacement of 17 mm after the 42% ground motion test was applied (Okazaki *et al.*, 2013). On the basis of the previous research (Yoo *et al.*, 2008), the FE model was adopted and 12,960 elements were used to conduct the nonlinear inelastic analysis. The local mesh density was increased toward the expected plastic regions and connections. A relative fine mesh (15 mm \times 20 mm, 25 mm \times 25 mm, and 25 mm \times 35 mm) was used near the beam-column interface,

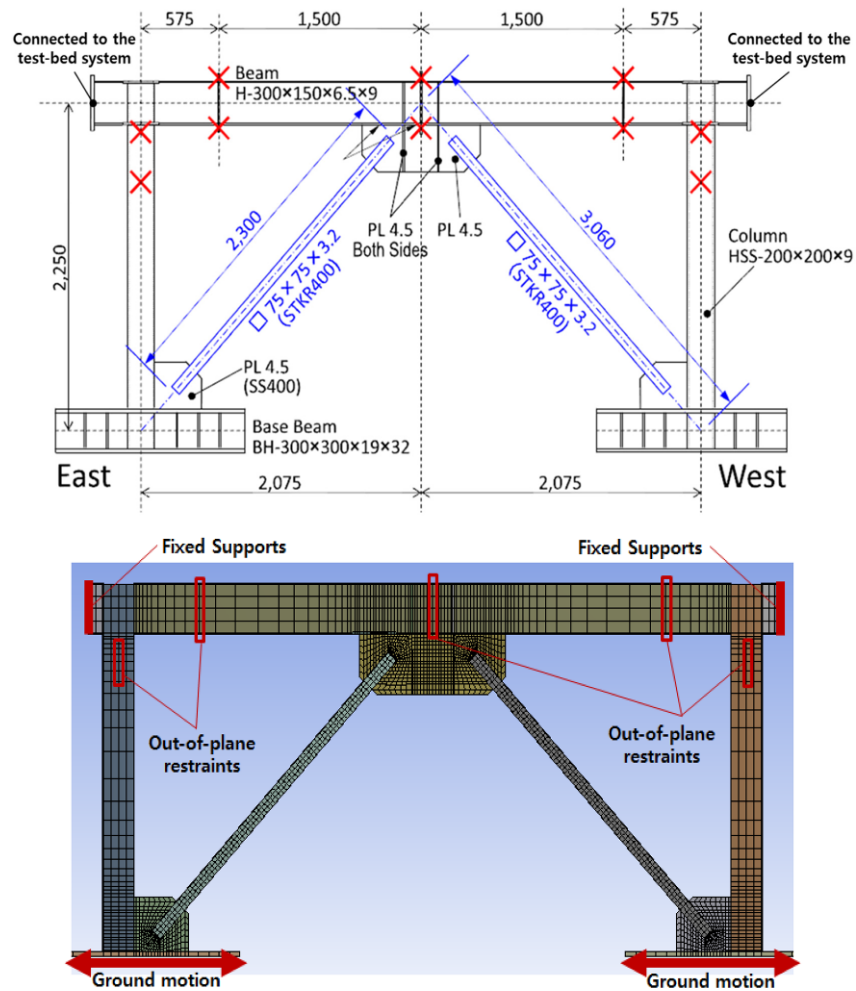


Figure 3. (a) Test specimen (Okazaki *et al.*, 2013); (b) finite element model configuration and boundary conditions.

Table 1. Material properties and geometry (Okazaki *et al.*, 2011)

Member	Designation	Size [mm]	Dimension [mm]	Fu [MPa]	Fu [MPa]	Elongation [%]
Brace	STKR400	HSS75×75×3.2	2,300 Long	383	452	36
Beam flange	SN400B	H-300×150×6.5×9	3,950 Long	327	456	27
Beam web				376	472	29
Column	BCR295	HSS200×200×9	2,550 Long	434	518	19
Gusset plate	SS400	middle	339×370	4.5 Thick	204	291
		corner	361×350			

the gusset plate connections and the middle of the brace, as illustrated in Fig. 3(b). A coarser mesh was used elsewhere, as only limited plastic deformations were expected.

4. Comparison of Experimentally Measured and Computed Responses

4.1. Global comparison

Detailed comparisons between experimentally observed and measured behaviors both at the local and global levels were made. These comparisons were then used to

verify that the theoretical predictions accurately represented the cyclic, inelastic system performance and properly simulated the local yield mechanisms. This was verified by comparing experimental results to the load-displacement responses of the developed analysis model.

The measured (Okazaki *et al.*, 2013) and simulated relations between the story shear and the lateral drift for the specimen are shown in Fig. 5. The FE model closely approximated all aspects of the measured response. On average, the errors for the maximum and minimum values of resistances are 0.59 and 1.74%, respectively.

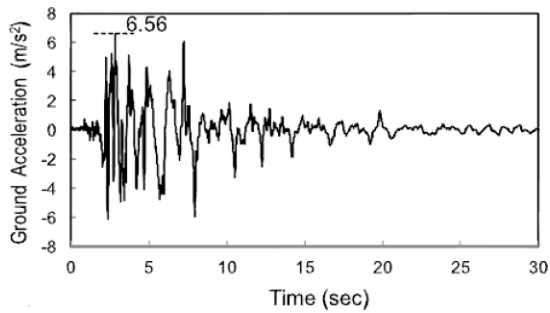


Figure 4. Ground motion: JR Takatori EW acceleration history (Okazaki *et al.*, 2013).

4.2. Local comparison

The analytical model also simulated the local behavior well. Figure 6 show observed (Okazaki *et al.*, 2013) and simulated yield patterns. In the Fig. 6(a) and 6(c), flaking of white wash indicated that the gusset plates had yielded. In terms of the equivalent stress of the analysis model, dark-colored areas, shown in Fig. 6(b), 6(d), are the yielding area based on the yield strength (204 MPa) of the gusset plates. Since the yield strengths of the beam and column (376 and 434 MPa, respectively) are much higher than that of the gusset plates, it is hard to say that the dark-colored areas of the equivalent stress of the beam and column are expected to yield. Both the experiments and analyses showed that significant out-of-plane deformation

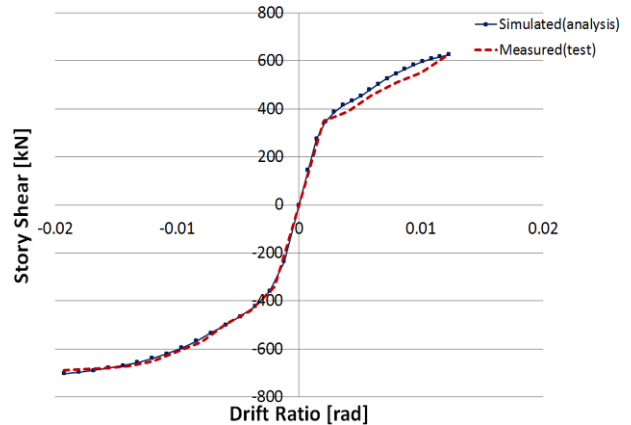


Figure 5. Measured (Okazaki *et al.*, 2013) and simulated relations between the story shear and the lateral drift.

and flexural yielding occurs within the gusset plate and the yielding does not occur in a straight line but forms in a curved band. The analysis accurately predicted the location and extent of this yielding.

4.3. Failure analysis

Evaluation of the stresses and strains at the critical locations, the middle of the brace and gusset plate weld, may lead to insight into the damage to and failure of the specimens. The analytically predicted inelastic strain state

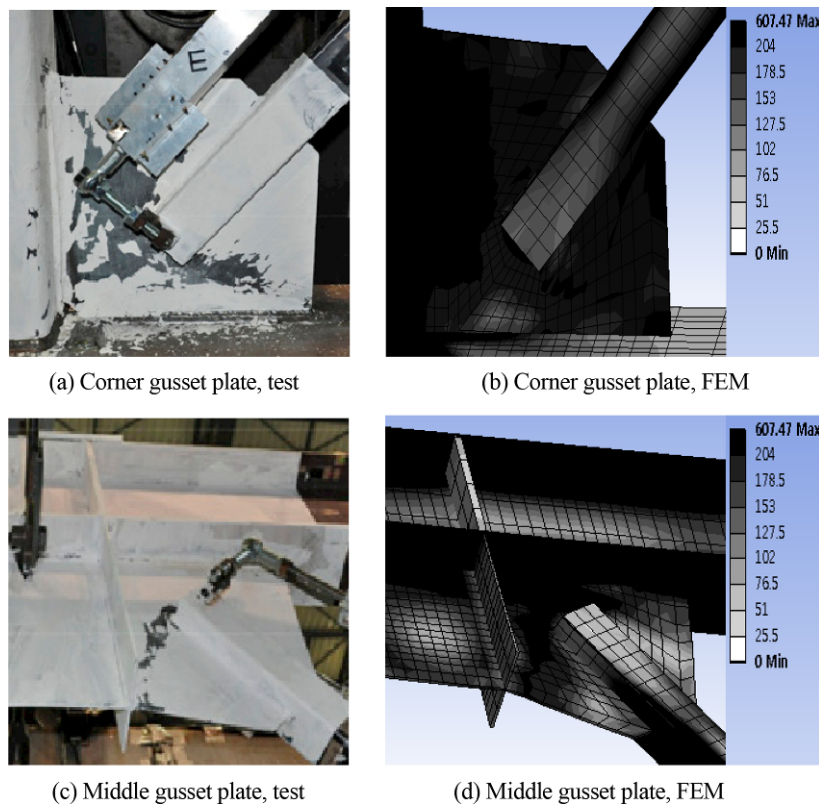


Figure 6. Typical yielding of gusset plate connecting east braces to frame.

was a logical index to use as indicators of the fracture of these locations. Yoo *et al.* (2008) used the equivalent plastic strain (ϵ_{eau}^{pl}) to evaluate the inelastic behavior and fracture potential of concentrically braced frame connections and braces. A similar approach was adopted as part of this study. The tearing and fracture noted during the tests were ductile. That is, cracks developed and lengthened prior to complete fracture. As a result, the ϵ_{eau}^{pl} was used as a primary indicator of fracture and tearing potential for the experimental test specimens at the middle of the brace and the interface gusset-plate welds (Yoo *et al.*, 2008). The ϵ_{eau}^{pl} was computed using the general von Mises equation:

$$\epsilon_{eau}^{pl} = \frac{1}{\sqrt{2}(1+\nu)} [(\epsilon_x^{pl} - \epsilon_y^{pl})^2 + (\epsilon_y^{pl} - \epsilon_x^{pl})^2 + (\epsilon_x^{pl} - \epsilon_x^{pl})^2 + \frac{2}{3}(\gamma_{xy}^{pl2} + \gamma_{yx}^{pl2} + \gamma_{xx}^{pl2})]^{1/2} \quad (4)$$

where ϵ_x^{pl} , ϵ_y^{pl} , ϵ_{xy}^{pl} , etc.=appropriate component strains
 ν =effective Poisson's ratio

The primary and preferred failure mode of the experimental CBF systems was ductile tearing and ultimate fracture of the braces. In the previous research (Yoo *et al.*, 2008), the ϵ_{eau}^{pl} values were between 0.271 and 0.306 at the frame deformation at which brace fracture occurred in the experiments. Thus, in this study, these values were applied to predict the time of brace fracture. Figure 7 shows the history of the equivalent plastic strain of the east brace and the brace fracture limit line in the analysis model. In the test (Okazaki *et al.*, 2013), the brace was fractured at the equivalent plastic strain of 0.018 rad, and the brace fracture point is as shown in Fig. 7. The time when the middle of the brace was fractured in the test and the time when the equivalent plastic strain reached the brace fracture limit line in the analysis model were exactly identical. This indicates that the analysis model

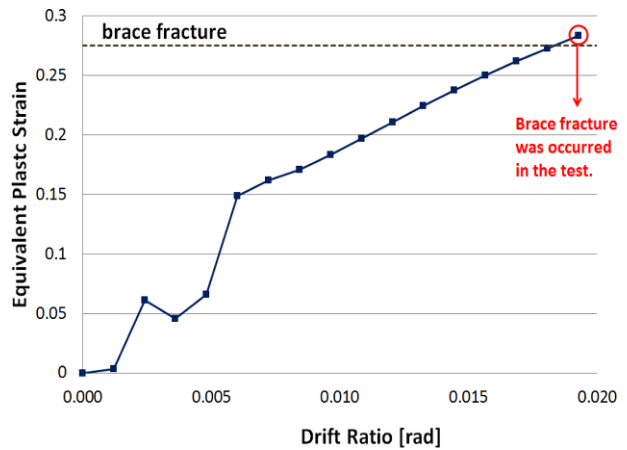


Figure 7. Equivalent plastic strain at the middle of the brace as function of drift range.

developed in this study can accurately predict the time of brace fracture.

5. Influence of Study Parameters

5.1. Parameters

Based on the analysis model verified above, 6 specimens were constructed in total to review the influence on inverted V-braced frames of the design methods for the cross section of beams and the clearance distance of gusset plates and the brief description of each specimen is shown in Table 2: In Specimen (1), the test object of the prior test (Okazaki *et al.*, 2013) and the FE model in Section 4 were the same. In Specimens (2), (3) and (4), the cross section of the beam was reduced to the size of which DCR (Demand-Capacity Ratio) was over 1.0. In Specimens (5) and (6), every condition is the same as Specimens (1) and (2) respectively, but the clearance distances of gusset plates were $8t_p$ elliptical clearance and $2t_p$ linear clearance respectively.

In Table 2, expected brace force is axial force calculated

Table 2. Parameters

Specimen	Gusset plate THK. [mm]	Clearance distance [mm]	Expected brace force			Vertical unbalanced force, V_u [kN]	Flexural capacity of beam [kN]	DCR for flexure (Demand-Capacity Ratio)
			Pt [kN]	Pc [kN]	0.3Pc [kN]			
(1) H-300×150×6.5×9-8TEC	4.5	235	342.02	209.10	62.73	205.31	221.07	0.9287
(2) H-298×149×5.5×8-8TEC	4.5	235	342.02	209.10	62.73	205.31	205.27	1.0002
(3) H-250×125×6.0×9-8TEC	4.5	235	342.02	207.77	62.33	204.54	178.52	1.1457
(4) H-200×100×5.5×8-8TEC	4.5	235	342.02	206.43	61.93	203.77	141.30	1.4421
(5) H-300×150×6.5×9-2TLC	9.0	161	342.02	225.23	67.57	201.75	221.07	0.9126
(6) H-250×125×6.0×9-2TLC	9.0	161	342.02	223.89	67.17	201.00	178.52	1.1259

Specimen : H-300×150×6.5×9 - 8TEC

Beam size Clearance type (8TEC: $8t_p$ elliptical clearance, 2TLC: $2t_p$ linear clearance)

where Pt = expected axial force on tensile brace

Pc = expected axial force on compressive brace

V_u = vertical unbalanced force calculated by Eq. (3)

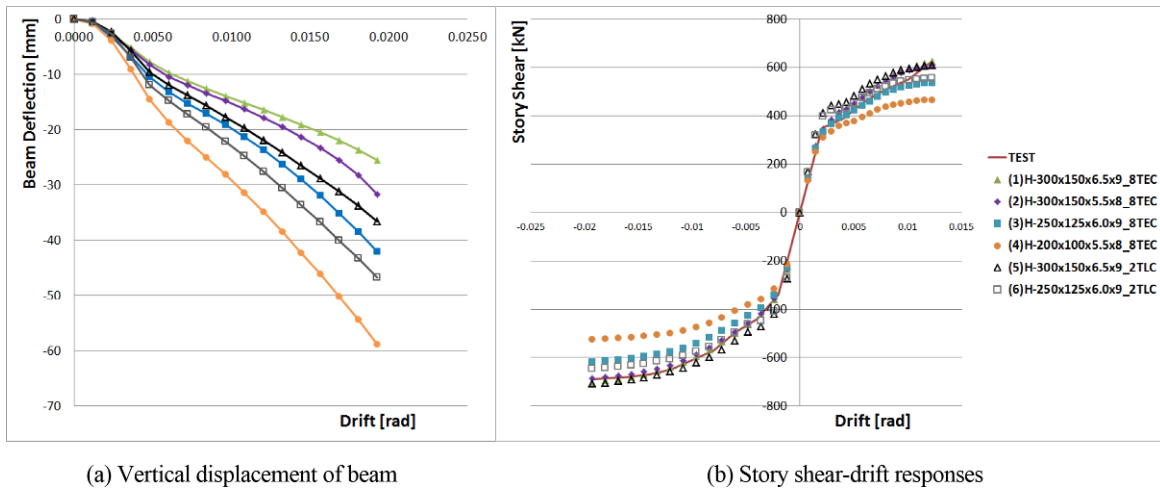


Figure 8. Global responses.

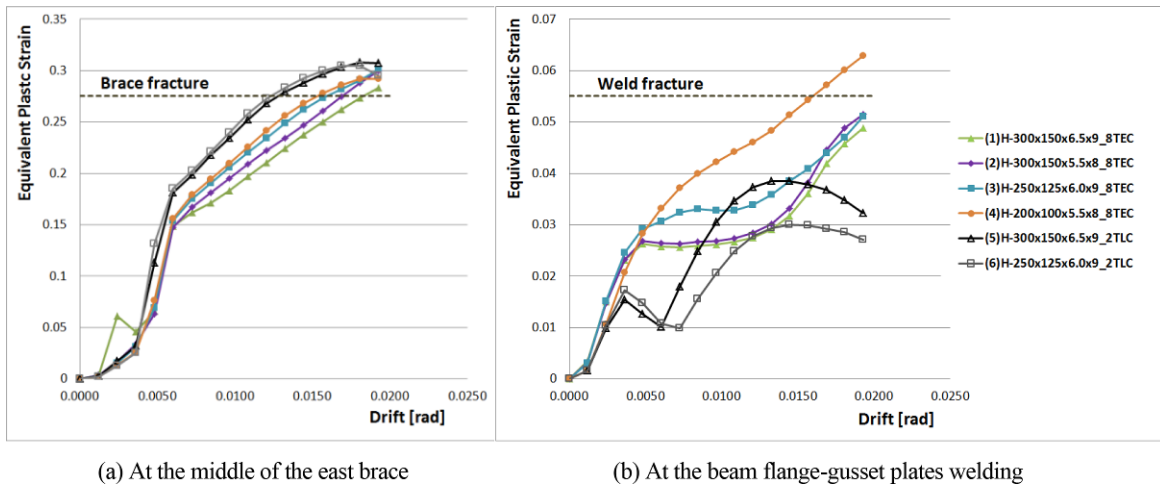


Figure 9. Equivalent plastic strain.

by the equation of the current AISC Design Provisions (2010a), and consequent vertical unbalanced force was calculated. The total length of the variation model was the same as 3,950 mm, and beams were subject to bending. It is possible to predict that plastic hinge can be created in the middle of the beam in the analysis model in Specimens (2), (3), (4) and (6) of which DCR is over 1.0. In every calculation in Table 2, strength coefficient was ignored, and flexural capacity was calculated in consideration of the influence of gusset plates. The reason why the gusset plates of Specimens (5) and (6) were twice thicker than those of other specimens was to satisfy the provision (AISC, 2010a) that the resisting force of the gusset plate calculated with the Whitmore section (Whitmore, 1952) shall be larger than the strength of the brace.

5.2. Results

Finite element analysis was conducted on the 6 specimens mentioned above using ANSYS. Figure 8(a) shows the changes in deflection of beam by transverse strain. As the

graph illustrates, the smaller the cross section of beams was, the larger the deflection in the middle of the beams was. As $2t_p$ linear clearance was applied to connections, the deflection in the middle of the beams became larger. This indicates that not just the cross section of the beams, but also the methods of designing connections have a big influence on the vertical load on the beams. Figure 8(b) shows the story shear-drift responses of frames. The smaller the cross section of the beams was, the smaller the transverse rigidity and strength of the frames were. However, the methods of designing connections did not have a big influence on the rigidity and strength of the frames within the same deflection range.

Using the equivalent plastic strain rate of the analysis models mentioned above, the types and times of frame fracture were evaluated. Figure 9(a) and 9(b) show the equivalent plastic strain responses at the middle of braces and at the welded connection between the beam flange and gusset plates respectively. The limit lines of brace fracture and weld fracture were obtained from an earlier

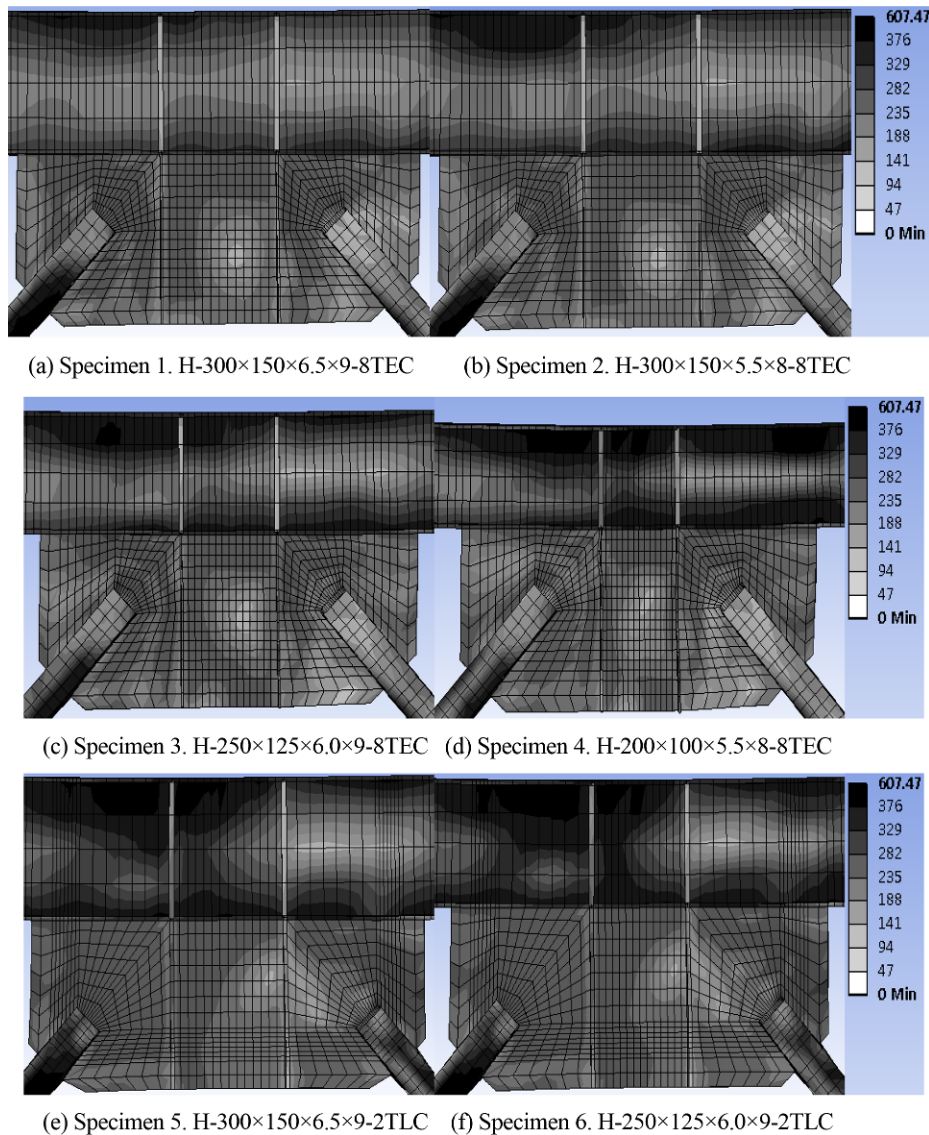


Figure 10. Equivalent stresses at the middle of the beam and gusset plates.

study (Yoo *et al.*, 2008). As shown in Fig. 9(a), the smaller the cross section of the beams was, the earlier the braces were fractured. In addition, when $2t_p$ linear clearance was applied to the connections, brace fracture occurred earlier. In particular, in the cases of Specimens (5) and (6) designed on the basis of the current standard that applied $2t_p$ linear clearance, their braces were fractured early, so that their frames were not able to support inelastic deformation enough. Figure 9(b) shows the equivalent plastic strain at the welded connection between the beam flange and gusset plates, and all the specimens except Specimen (4) failed to reach the range of weld fracture. In the case of Specimen (4), compared to Fig. 9(a) and 9(b), brace fracture occurred earlier than the fracture of welded connections, and thus it will be possible to say that the final failure mode is the fracture at the middle of the braces. In other words, the failure mode of

all the specimens is the fracture at the middle of the braces.

The equivalent plastic strain at the middle of the beams was reviewed in order to locally evaluate the influence of vertical unbalanced force on the middle of the frames, and the results are shown in Fig. 10. The figure shows the stress extracted on the basis of 376 MPa of the yield strength of the beam web at 0.013% of drift, and for visual comparison, the areas of deformation was magnified to 1.5 times. The braces on the left show the time of tension, and those on the right side show the time of compression. As shown in Fig. 10(a)~10(d), the smaller the cross section of the beams was, the larger the yield area of the beam webs was due to vertical unbalanced force. Table 3 is the list of the analysis results of the specimens. As shown in the table, the differences in the vertical unbalanced force generated at the middle of the

Table 3. The results of parametric analysis

Specimen	Strength [kN]	Drift range [rad]	Tensile brace			Compressive brace			Vertical unbalanced force		
			Pt _{FEM} [kN]	Pt _{AISC} [kN]	Pt _{FEM} /Pt _{AISC} [%]	Pc _{FEM} [kN]	Pc _{AISC} [kN]	Pc _{FEM} /Pc _{AISC} [%]	Vn _{FEM} [kN]	Vn _{AISC} [kN]	Vn _{FEM} /Vn _{AISC} [%]
(1) H-300×150×6.5×9-8TEC	-706 ~618	-0.0116~0.0193 (Total 0.0309)	322	342	94	84	209	40	176	205	86
(2) H-300×150×5.5×8-8TEC	-681 ~598	-0.0108~0.0181 (Total 0.0289)	320	342	94	84	209	40	174	205	85
(3) H-250×125×6.0×9-8TEC	-609 ~526	-0.0101~0.0169 (Total 0.0270)	311	342	91	92	208	44	161	205	79
(4) H-200×100×5.5×8-8TEC	-517 ~452	-0.0094~0.0157 (Total 0.0251)	306	342	90	89	206	43	158	204	78
(5) H-300×150×6.5×9-2TLC	-672 ~565	-0.0080~0.0133 (Total 0.0213)	341	342	100	101	225	45	177	202	88
(6) H-250×125×6.0×9-2TLC	-617 ~523	-0.0080~0.0133 (Total 0.0213)	332	342	97	123	224	55	153	201	76
Average	-	-	-	-	94	-	-	45	-	-	82

where Pt_{FEM}, Pc_{FEM}, Vn_{FEM}, = analytical results

Pt_{AISC}, Pc_{AISC}, Vn_{AISC}, = expected tabforces calculated by AISC Seismic Provisions (2010b)

beams in analyzing were not significant. Thus, it is natural that the yield areas of the beam webs were bigger in Specimens (3), (4) and (6) since the bending strength of the beams on vertical unbalanced force was small. In addition, in the cases of Specimens (5), (6), 2t_p linear clearance was applied, and their yield areas were larger than those with elliptical clearance applied.

The analysis results of the specimens were summarized in Table 3. When Specimens (1) and (5); and Specimens (3) and (6) were compared respectively -that is the comparison between the methods of designing connections- Specimens (1) and (3) with elliptical clearance applied showed an approximately 40% larger inelastic deformation capacity than Specimens (5) and (6) with linear clearance applied. This indicates that the proposed methods of designing connections with elliptical clearance applied (Lehman *et al.*, 2008; Roeder *et al.*, 2011) have better earthquake-resistant performance in inverted V-braced frames than the current standards. The thickness of gusset plates using elliptical clearance can be reduced in half compared to those using linear clearance, and at the same time the earthquake-resistant performances of the entire frames can be improved.

The analysis results indicate that the vertical unbalanced force predicted under the current AISC Seismic Provisions (2010b) is significantly more conservative than the real vertical unbalanced force obtained with the analysis model. In Table 3, the values calculated under the current standards (subscript AISC in Table 3) and the values extracted from the analysis results (subscript FEM in Table 3) were compared in terms of the axial force of tension and compression braces, and its vertical unbalanced force. Under the analysis model, tension brace was under the load of approximately 94% of the expected tensile

force, and compression brace was under the load of approximately 45% of the expected compression force. The results are conflicting with the Eq. (3) that calculates vertical unbalanced force with full yield tension brace and compression brace having the post-buckling strength of 30% of compression strength. The final results show that the vertical unbalanced force obtained from the analysis results was approximately 82% of the vertical unbalanced force that was calculated using the equation of the current standards, which is the evidence that the method of calculating vertical unbalanced force under the current standards is conservative.

6. Conclusions and Recommendations for Future Work

This study aimed to evaluate the influence of the methods of designing clearance distance of connections of gusset plates on the earthquake-resistant performances of inverted V-braced frames, and the vertical unbalanced force of inverted V-braced frames. To do so, 2 variables were applied to 6 specimens for finite element analysis, and the results of this study are as follows:

(1) The validity of the finite element analysis models was verified through the comprehensive comparison using the story shear force-deformation curves obtained from the test results of inverted V-braced frames (Okazaki *et al.*, 2013), and through the local comparison using equivalent plastic strain and equivalent stress.

(2) The Balanced Design Procedure (BDP), a method of designing CBFs (Concentrically Braced Frames), and Ntp elliptical clearance were introduced, and their applicability to the gusset plate connections of inverted V-braced frames was evaluated. While the analysis

models with Ntp elliptical clearance applied showed good earthquake-resistant performance, braces were fractured early in the analysis model with 2tp linear clearance applied as stated in the current standards.

(3) As indicated in the analysis results of variations, the smaller the cross section of beams in inverted V-braced frames was, the lower the earthquake-resistant performances were, including the increased deflection at the middle of beams; the decreased rigidity and strength of frames; and the early fracture of braces.

(4) Using the analysis results of all the variations, the real vertical unbalanced force applied to the beams of inverted V-braced frames was studied, and it was approximately 82% of the predicted results calculated using the vertical unbalanced force equation of the current standards.

(5) The analysis results of equivalent plastic strain indicated that the area most affected by vertical unbalanced force in beams was not the middle of beams, but the width end of gusset plates. In addition, depending on the methods of designing the clearance distance of gusset plates, the tension and compression forces of braces were different, which indicates that these factors associated with vertical unbalanced force should be considered in designing members.

Through this study, several expected effects were obtained as follows:

(1) This study presented analysis models that can accurately evaluate earthquake behaviors in inverted V-braced frames including rigidity, strength, inelastic deformation capacity, failure mode, the time of fracture, etc.

(2) The results of this study corresponded to the results of earlier studies (Lehman *et al.*, 2008; Roeder *et al.*, 2011) in which the performance and applicability of elliptical clearance to inverted V-braced frames were excellent. When this is applied to the real design of frames, more compact connections can be achieved and at the same time the earthquake-resistant performance of frames can be improved.

(3) This study highlighted the importance of considering vertical unbalanced force in the design of inverted V-braced frames, and determining the proper cross-section size of beams.

(4) Through this study, it was found that the current standards overestimate vertical unbalanced force, and it was suggested to reconsider its equation of the current standards, and to consider critical points in vertical unbalanced force as well as differences in the axial force of braces depending on the methods of designing clearance distance.

This study is expected to be used as the basis for designing inverted V-braced frames. In the follow-up studies, the objectivity and validity of the results of this study need to be secured through experimental and analytical approaches to a variety of variations of inverted

V-braced frames. It will be also necessary to develop an equation for the accurate prediction of vertical unbalanced force through quantitative and repeated verification procedures.

Acknowledgments

This work was supported by the National Research Foundation of Korea (NRF) grant funded by the Korean Government (Ministry of Science, ICT & Future Planning) [NRF-2012R1A1A1002843].

References

- American Institute of Steel Construction (AISC). (2010a). *Seismic Provisions for Structural Steel Buildings*. ANSI/AISC 341-10, Chicago, IL
- American Institute of Steel Construction (AISC). (2010b). *Specification for Structural Steel Buildings*. ANSI/AISC 360-10, Chicago, IL.
- ANSYS. (2012) "ANSYS multiphysics, Ver. 14.5." ANSYS Inc., Cannonsburg, PA.
- Astaneh-Asl, A., Goel, S.C., and Hanson, R.D. (1986). "Earthquake-resistant design of double angle bracing." *Engineering Journal*, 23(4), pp. 133-147.
- Bruneau, M., Uang, C.M., and Sabelli, R. (2011). *Ductile design of steel structures*, 2nd Ed. McGrawHill, NY.
- Khatib, I.F., Mahin, S.A., and Pister, K.S. (1988). *Seismic Behavior of Concentrically Braced Steel Frames*. Report UCB/EERC-88/01, Earthquake Engineering Research Center, University of California.
- Lehman, D.E., Roeder, C.W., Herman, D., Johnson, S., and Kotulka, B. (2008). "Improved seismic performance of gusset plate connections." *Journal of Structural Engineering*, ASCE, 134(6), pp. 890-901.
- Nakamura, Y., Uehara, F., and Inoue, H. (1996). *Waveform and its analysis of the 1995 Hyogo-ken-Nambu earthquake II*. JR Earthquake Information No. 23d, UrEDAS R&D Promotion Dept., Railway Technical Research Institute, Tokyo.
- Okazaki, T., Lignos, D.G., Hikino, T., and Kajiwara, K. (2013). "Dynamic Response of a Chevron Concentrically Braced Frame." *Journal of Structural Engineering*, ASCE, 139(4), pp.515-525.
- Okazaki, T., Lignos, D.G., Hikino, T., and Kajiwara, K. (2010). "Dynamic Response of a Steel Concentrically Braced Frame." *Structures Congress 2011*, ASCE, pp. 950-959.
- Roeder, C.W., Lumpkin, E.J., and Lehman, D.E. (2011). "A balanced design procedure for special concentrically braced frame connections." *Journal of Constructional Steel Research*, 67(11), pp.1760-1772.
- Whitmore, R.E. (1952). *Experimental Investigation of Stresses in Gusset Plates*. Bulletin No.16, Engineering Experiment Station, University of Tennessee.
- Yoo, J.H., Roeder, C.W., and Lehman, D.E. (2008). "Analytical Performance Simulation of Special Concentrically Braced Frames." *Journal of Structural Engineering*, ASCE, 134(6), pp. 881-889.